

Light curve of a hotspot on equatorial orbit around Kerr black hole surrounded by reflective firewall

Sudipta Hensh,^{1,*} Jan Schee,^{1,†} and Zdeněk Stuchlík^{1,‡}

¹*Research Centre for Theoretical Physics and Astrophysics,
Institute of Physics, Silesian University in Opava,
Bezručovo náměstí 13, CZ-74601 Opava, Czech Republic*

(Dated: March 1, 2022)

The light curve of an isolated bright spot in a Keplerian orbit is studied to investigate the signature of the firewall around the event horizon of the black hole. An increase in total observed flux is found. In addition to that, for firewall case comparatively a longer time radiation is observed.

1. INTRODUCTION

Recent technological advancements in getting signatures of astrophysical events has been remarkable in the last decade. Gravitational wave observations by LIGO/VIRGO/KAGRA confirmed the primary existence of the black hole [1]. On the other hand the first image of galactic center black hole of M87 confirmed the existence of the super-compact object but till now not able to resolve completely between black hole and black hole mimickers [2–7]. So, the nature of the black hole is still unknown. Recently, we have also seen first polarized image of the black hole in the center of the M87 galaxy [8, 9]. Next generation gravitational waves detectors and event horizon telescope would be able to shed some light on the strong field signatures of gravity and may test the nature of the black hole.

Vacuum fluctuations produce particle anti-particle entangled pair and they annihilate very rapidly because of short lifespan. When this pair production occurs in the close vicinity of the event horizon then one of them falls into the black hole and the other one escapes to the infinity as Hawking radiation [10]. Information loss in Hawking radiation is still an active area of research. A proposal to avoid information loss in Hawking radiation is to give up on Einstein's principle of equivalence by considering that the in-falling observer would observe a pile of high-energy particle in the close vicinity of the horizon; namely firewall [11].

The existence of the firewall would basically appear in the strong field signatures that we can observe due to astrophysical events involving black holes. This can be in two possible ways; either in the gravitational wave emission or in the observed electromagnetic emissions. In this article, our intention is to investigate the latter. We are interested in observing signatures of firewall in the electromagnetic spectrum of a radiating hotspot. Any intrinsic variability in the local emission from the innermost region of the accretion disk could influence the observed X-ray variability [12]. The observational signatures of a corotating spot in accretion disk is studied in [13]. While radiation from hotspots in extreme Reissner-Nordstrom black hole is investigated in [14].

Detection of hot spot orbiting in a stable circular orbit around our galactic center black hole SgrA* by Gravity Collaboration [15] has introduced a lot of curiosity in the scientific community to model hot spot. There are many efforts available in the literature to study the hot spot. While we can not do justice to mention all the efforts, here we refer to some efforts such as [16–23]. A work dedicated to distinguish between the black holes and worm holes using hot spot can be found in [24]. While the model of hot spot from plasma microphysics is still an active area of research, our goal in this article is not to understand the underlying microphysics that governs the formation of hot spot but to focus on observational imprints of the firewall on the electromagnetic spectrum.

In Sec-2, we describe the governing equations of motion that uniquely determine the path traversed by the photon i.e. geodesic. Next in Sec-3, we describe our firewall model considering which this investigation is done and ray-tracing in the presence of the firewall. The constructions of the light curve is described and comparison plot of the light curve is demonstrated in Sec-4. In Sec-5, a summary of the whole analysis is presented. Throughout the paper, we consider $(-, +, +, +)$ signatures and geometrical system of units i.e. $G = c = 1$.

* f170656@fpf.slu.cz, sudiptahensh2009@gmail.com

† jan.schee@physics.slu.cz

‡ zdenek.stuchlik@physics.slu.cz

2. EQUATIONS OF MOTION

The spacetime interval of Kerr geometry in Boyer-Lindquist coordinates read

$$ds^2 = - \left(1 - \frac{2Mr}{\Sigma} \right) dt^2 + \frac{\Sigma}{\Delta} dr^2 + \Sigma d\theta^2 + \frac{A}{\Sigma} \sin^2 \theta d\phi^2 - \frac{4ar}{\Sigma} \sin \theta dt d\phi \quad (1)$$

where

$$\Delta = r^2 - 2Mr + a^2, \quad (2)$$

$$\Sigma = r^2 + a^2 \cos^2 \theta, \quad (3)$$

$$A = (r^2 + a^2)^2 - a^2 \Delta \sin^2 \theta. \quad (4)$$

For numerical advantages we use new radial and new latitudinal coordinates defined by $u \equiv 1/r$ and $m \equiv \cos \theta$. Following Hamilton-Jacobi separation of variable procedure one can get easily Carter equations of motion. The equations of motion of photon 4-momentum k^μ are given by

$$\Sigma k^t = aQ(l, m, a) + \frac{(1 + u^2 a^2)P(u, l, a)}{u^2 \Delta}, \quad (5)$$

$$\Sigma k^u = \pm \sqrt{U(u, l, q, a)}, \quad (6)$$

$$\Sigma k^m = \pm \sqrt{M(m, l, q, a)}, \quad (7)$$

$$\Sigma k^\phi = \frac{Q(l, m, a)}{1 - m^2} + \frac{aP(u, l, a)}{\Delta}, \quad (8)$$

with $l \equiv -k_\phi/k_t$ and $q \equiv \mathcal{C} - l^2$ (\mathcal{C} is Carter separation constant) being constants of motion and we have defined

$$Q(l, m, a) \equiv l - a(1 - m^2), \quad (9)$$

$$P(u, l, a) \equiv \frac{(1 + u^2 a^2)}{u^2} - la, \quad (10)$$

$$U(u, l, q, a) \equiv 1 + (a^2 - l^2 - q)u^2 + 2[(a - l)^2 + q]u^3 - a^2 q u^4, \quad (11)$$

$$M(m, l, q, a) \equiv q + (a^2 - l^2 - q)m^2 - a^2 m^4. \quad (12)$$

Introducing new affine parameter by re-scaling as

$$\frac{d}{d\lambda'} \equiv \Sigma \frac{d}{d\lambda}. \quad (13)$$

With this new affine parameter equations (5)-(8) reads

$$k^t = aQ(l, m, a) + \frac{(u^2 + a^2)P(u, l, a)}{u^2 \Delta}, \quad (14)$$

$$k^u = \pm \sqrt{U(u, l, q, a)}, \quad (15)$$

$$k^m = \pm \sqrt{M(m, l, q, a)}, \quad (16)$$

$$k^\phi = \frac{Q(l, m, a)}{1 - m^2} + \frac{aP(u, l, a)}{\Delta}. \quad (17)$$

In order to deal with the square root in equations (15) and (16), we make transition to second order differential equations, reading

$$\frac{dk^u}{d\lambda'} = \frac{1}{2} \frac{dU}{du}, \quad (18)$$

$$\frac{dk^m}{d\lambda'} = \frac{1}{2} \frac{dM}{dm}. \quad (19)$$

3. RAY-TRACING AND REFLECTION OFF THE FIREWALL

We consider firewall as a reflecting surface situated at $r_f = r_h + \epsilon$ i.e. just above the event horizon (r_h) and in our model $\epsilon = 10^{-4}M$. To keep the problem simple and understand qualitatively we have considered the firewall as a perfect reflector and the source of the radiation is only from the hotspot. In addition to that we also assume that the hotspot is geometrically thin and optically thick. In our model, we are also considering that the hotspot is laying on the equatorial plane maintaining a circular orbit and having a finite extension i.e. dr .

Here we are using so called backward-raytracing method using this technique one can trace the rays from the detector location to the source of emission. At first, we construct a 2-dimensional photographic plate and the coordinate (α, β) determines the location of the pixel on the photographic plate.

Each geodesic can be determined by two parameters (α, β) tightly connected with impact parameters (l, q) . The relation between the photographic plate coordinate and the constants of motion reads [25]

$$\alpha = \frac{l}{\sin \theta_o}, \quad (20)$$

$$\beta^2 = q + \cos^2 \theta_o \left(a^2 - \frac{l^2}{\sin^2 \theta_o} \right), \quad (21)$$

where θ_o is the inclination angle of the observer.

In order to determine the origin of the observed photon we construct its geodesics taking following steps:

- First we estimate the range of the photographic plate coordinates by taking projection of the whole black hole-hotspot system onto the observer's 2-dimensional sky.
- Then we divide the photographic plate $(\alpha - \beta)$ to finite pixels. For a given pixel $\alpha \in [\alpha_{min}, \alpha_{max}]$ and $\beta \in [\beta_{min}, \beta_{max}]$ determine l and q from equations (20) and (21).
- Next, we calculate the turning point u_t i.e. when radial velocity $U(u_t; l, q, a) = 0$ and turning points those occur in between the radius of the outer edge of the hotspot, r_{rmax} and radius of the event horizon, r_h are of our interest. This condition can be expressed as $u_t > u_{max} \equiv 1/r_{max}$ and $u_t < u_h \equiv 1/r_h \equiv (1 + \sqrt{1 - a^2})^{-1}$.
- In order to be computationally efficient, assuming the hotspot expands spans between r_1 and r_{max} , we determine the maximal meaningful value of the affine parameter λ_{max} as

$$\lambda_{max} = \begin{cases} \int_{u_o}^{u_h} \frac{du}{\sqrt{U(u; l, q, a)}} & \text{for } n_u = 0, \\ \int_{u_o}^{u_t} \frac{du}{\sqrt{U(u; l, q, a)}} + \int_{u_{max}}^{u_t} \frac{du}{\sqrt{U(u; l, q, a)}} & \text{for } n_u = 1, \end{cases} \quad (22)$$

where n_u indicates number of existing turning points along the geodesics (in the case of null geodesics we have two possibilities $n_u = 0$, indicating that there is no turning point and $n_u = 1$ indicating that there is one turning point).

- To get the geodesic we solve equations (14), (17), (18), (19) with the initial conditions at $\lambda = 0$ as

$$t(0) = 0, \quad (23)$$

$$u(0) = u_o, \quad (24)$$

$$m(0) = m_o, \quad (25)$$

$$\phi(0) = 0, \quad (26)$$

$$k^u(0) = \sqrt{U(u_o; l, q, a)}, \quad (27)$$

$$k^m(0) = \text{Sign}(\beta) \sqrt{M(m_o; l, q, a)}, \quad (28)$$

where $u_o = 1/r_o$ is the distance at which observer is located, and $m_o = \cos \theta_o$ is the inclination angle of the observer.

- Now the procedure splits into two cases: one with no turning point and the other with a turning point.

If there is no turning point i.e. $n_u = 0$ then we integrate equations of motion down to the horizon where the solution reads

$$t(\lambda_{max}) = t_h , \quad (29)$$

$$u(\lambda_{max}) = u_h , \quad (30)$$

$$m(\lambda_{max}) = m_h , \quad (31)$$

$$\phi(\lambda_{max}) = \phi_h , \quad (32)$$

$$k^u(\lambda_{max}) = k_h^u , \quad (33)$$

$$k^m(\lambda_{max}) = k_h^m . \quad (34)$$

We apply to this propagation vector perfect (energy and angular momentum are conserved) reflection by converting the radial component of the momentum from global coordinate (GC) to the locally non-rotating frame (LNRF) apply reflection and then switch back to the GC frame as given below

$$k_h^u \xrightarrow{\text{LNRF}} k_h'^u \xrightarrow{\text{Reflection}} -k_h'^u \xrightarrow{\text{GC}} k_h''^u . \quad (35)$$

So the new initial conditions read

$$t(0) = t_h , \quad (36)$$

$$u(0) = u_h , \quad (37)$$

$$m(0) = m_h , \quad (38)$$

$$\phi(0) = \phi_h , \quad (39)$$

$$k^u(0) = k_h''^u , \quad (40)$$

$$k^m(0) = k_h^m . \quad (41)$$

We determine new maximal value of the affine parameter

$$\lambda_{max} = \int_{u_h}^{u_{max}} \frac{du}{\sqrt{U(u; l, q, a)}} . \quad (42)$$

Then we integrate the system of differential equations (14), (17), (18), (19) and check the intersection between the rays and the hotspot.

If there is a turning point $n_u = 1$ in this case the geodesics is not divided into segments. We integrate system of diff equations (14), (17), (18), (19) down to $\lambda = \lambda_{max}$ and check for intersection with the hotspot.

For each intersection radius of emission r_e is determined along with corresponding frequency shift g i.e. the ratio of the observed frequency ν_o to the emitted frequency ν_e using the formula

$$g = \frac{\nu_o}{\nu_e} = \left[1 - \frac{2}{r_e} (1 - a\Omega_e)^2 - (r_e^2 + a^2)\Omega_e^2 \right]^{1/2} (1 - l\Omega_e)^{-1} , \quad (43)$$

where Ω_e is the velocity of the photon orbiting in a Keplerian orbit which can be written as

$$\Omega_e = \frac{1}{r_e^{3/2} + a} . \quad (44)$$

4. LIGHT CURVE

The local emission profile of the hotspot in our model is given by

$$I_e = I_0 r_e^{-p} , \quad (45)$$

where I_0 is a normalization constant and r_e is the radial location of local emission. As we are assuming that there is no energy loss while travelling from the emission point to the observer, so the observed intensity reads

$$I_o = g^4 I_e . \quad (46)$$

$a \backslash \theta_o$	30°	45°	60°	$a \backslash \theta_o$	30°	45°	60°
0.1	2.75311	2.78655	2.89336	0.1	2.75723	2.85983	2.89858
0.3	2.56454	2.59181	2.59576	0.3	2.56314	2.62253	2.57782
0.5	3.22061	3.26359	3.27170	0.5	2.79891	3.22683	3.29580
0.7	2.74059	2.76949	3.77723	0.7	2.79994	2.80763	3.35492
0.9	5.68790	5.76954	6.41901	0.9	5.67351	5.82698	6.04234
0.998	16.16741	15.91805	16.42907	0.998	16.18878	15.81999	16.45374

TABLE I. Fractional change in the total flux, $\frac{(\text{Total Flux}_{\text{Firewall}} - \text{Total Flux}_{\text{Kerr}}) \times 100}{\text{Total Flux}_{\text{Kerr}}}$ due to reflection of the firewall for hotspot location $r = r_{\text{ISCO}}$ with extension, $dr = 0.5\text{M}$ (on the left table) and $dr = 1\text{M}$ (on the right table).

$a \backslash \theta_o$	30°	45°	60°	$a \backslash \theta_o$	30°	45°	60°
0.1	2.70518	2.88087	3.05934	0.1	3.03606	2.97446	3.18057
0.3	2.75398	2.88230	2.95083	0.3	2.88109	2.80441	2.86375
0.5	2.88655	3.04380	3.20818	0.5	3.06993	3.00101	3.20856
0.7	3.01764	3.01958	2.91420	0.7	3.00406	2.91969	2.93161
0.9	3.74769	4.19611	4.17147	0.9	3.78371	4.09081	4.21665
0.998	14.83085	14.91613	14.91858	0.998	14.42621	14.63764	14.84966

TABLE II. Fractional change in the total flux, $\frac{(\text{Total Flux}_{\text{Firewall}} - \text{Total Flux}_{\text{Kerr}}) \times 100}{\text{Total Flux}_{\text{Kerr}}}$ due to reflection of the firewall for hotspot location $r = 2r_{\text{ISCO}}$ with extension, $dr = 0.5\text{M}$ (on the left table) and $dr = 1\text{M}$ (on the right table).

Lets us consider that a photon takes time Δt to reach the observer from the hotspot which is located at the radius r_e and azimuthal angle ϕ . Then the total coordinate time it takes can be written as

$$t = \Delta t + \frac{\phi}{\Omega_e}. \quad (47)$$

One can get the light curve after sorting the photons according to their arrival time and plotting the intensity (I_o) vs time (t) curve.

5. DISCUSSION

We performed ray-tracing simulations to construct the geodesic of the photons which travel up to the observer from the hotspot and then considering the local power-law emission profile as given in (45) with the choice $I_0 = 1$ and $p = 1.5$. In the simulations, four representative values of the orbit of the hot spot $r = r_{\text{ISCO}}, 2r_{\text{ISCO}}, 3r_{\text{ISCO}}, 4r_{\text{ISCO}}$, three values of observer's inclination angle, $\theta_o = 30^\circ, 45^\circ, 60^\circ$, and two values of radial extension of the hot spot $dr = 0.5\text{M}, 1\text{M}$ are considered.

In case of Kerr black hole, some fraction of photons which emit from the hotspot may lost down to the horizon of the black hole forever. If the event horizon is fully screened by the firewall then emitted photon would suffer reflection when it hits the firewall. A fraction of these photons would travel up to the observer and contribute in the observed flux. As expected due to the reflection of the firewall the total flux increases. The comparison between the Kerr

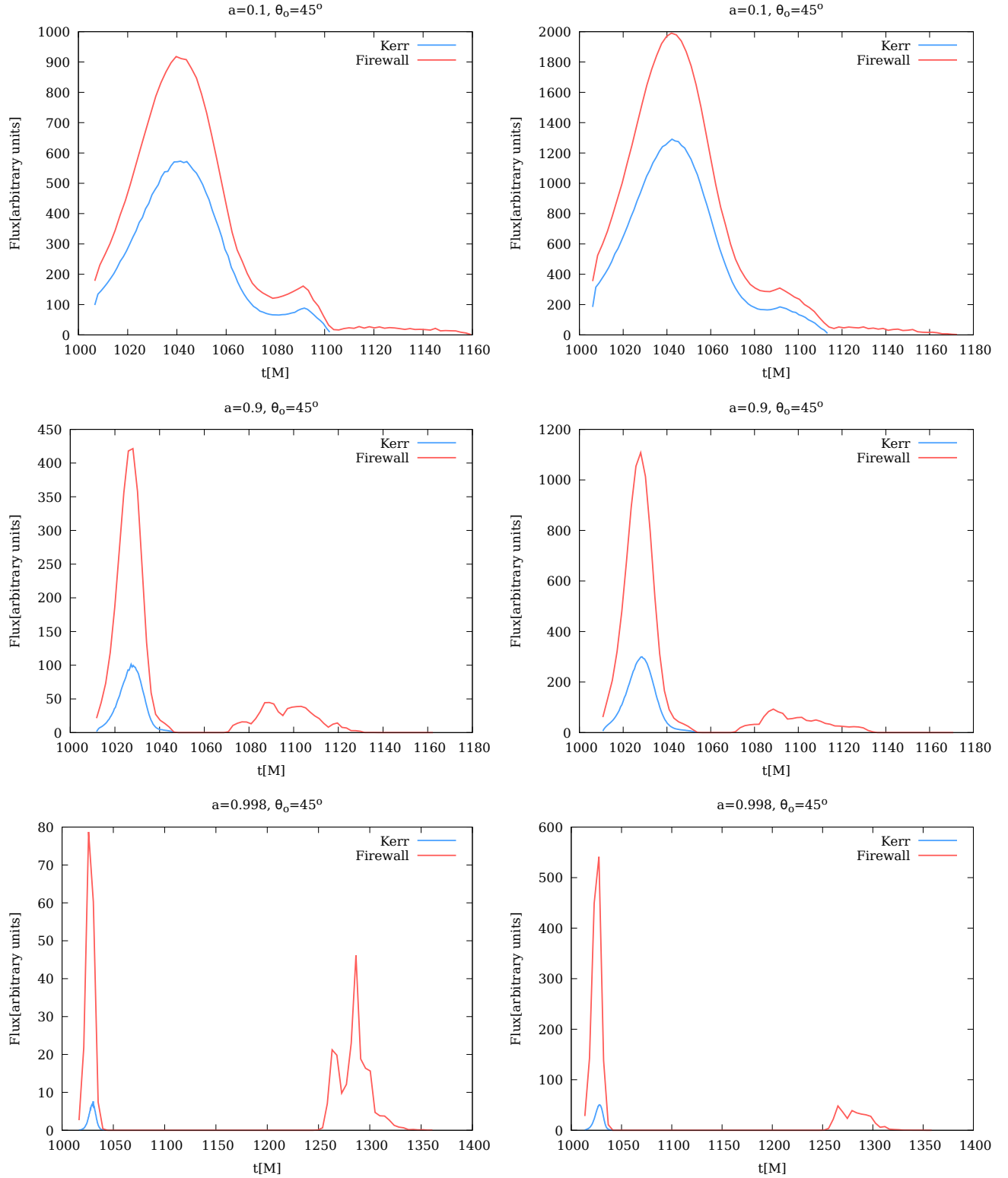


FIG. 1. Comparison of the light curve for hotspot extension, $dr = 0.5M$ (on the left column) and $dr = 1M$ (on the right column). The hotspot location is at radius $r = r_{\text{ISCO}}$.

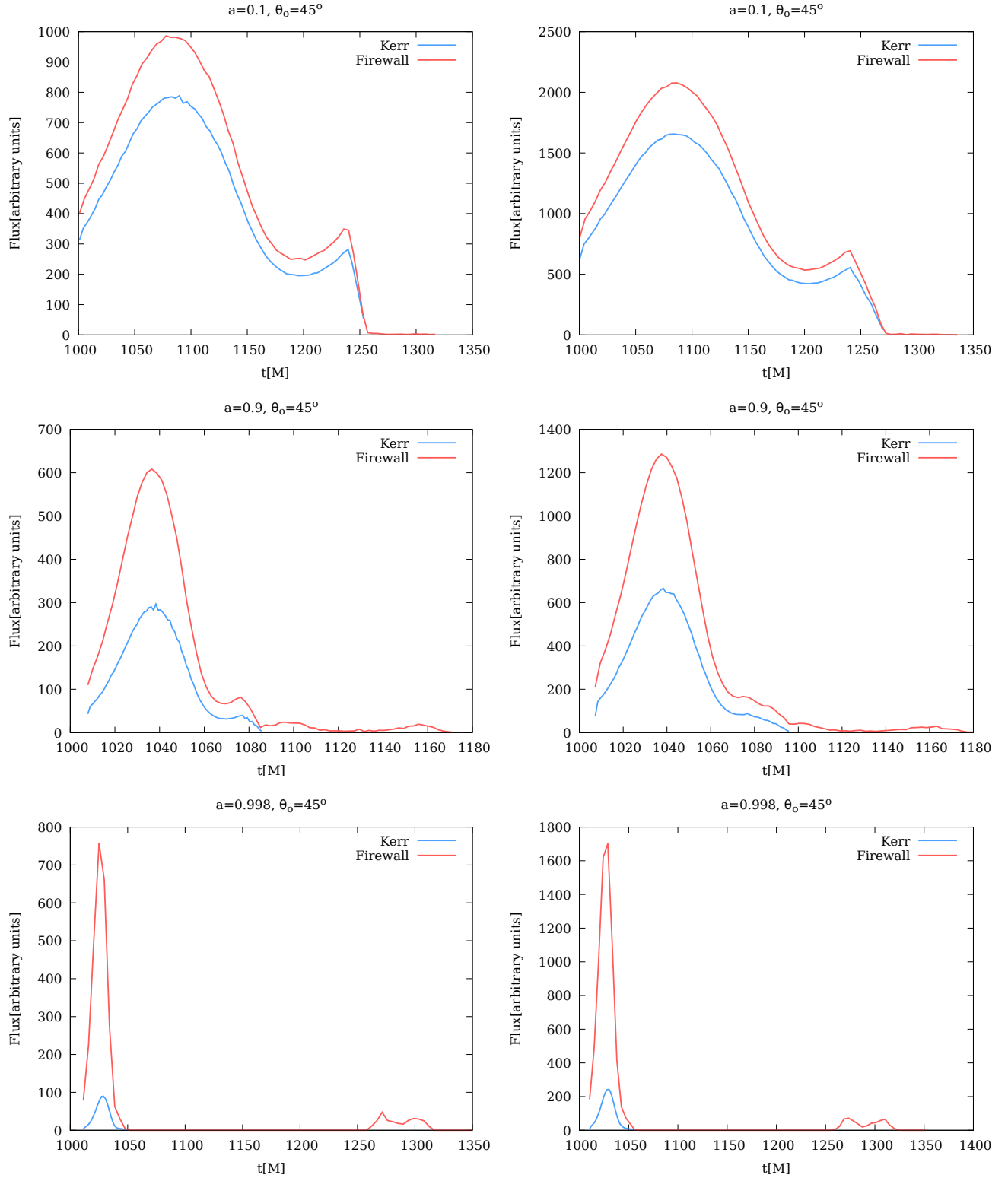


FIG. 2. Comparison of the light curve for hotspot extension, $dr = 0.5M$ (on the left column) and $dr = 1M$ (on the right column). The hotspot location is at radius $r = 2r_{\text{ISCO}}$.

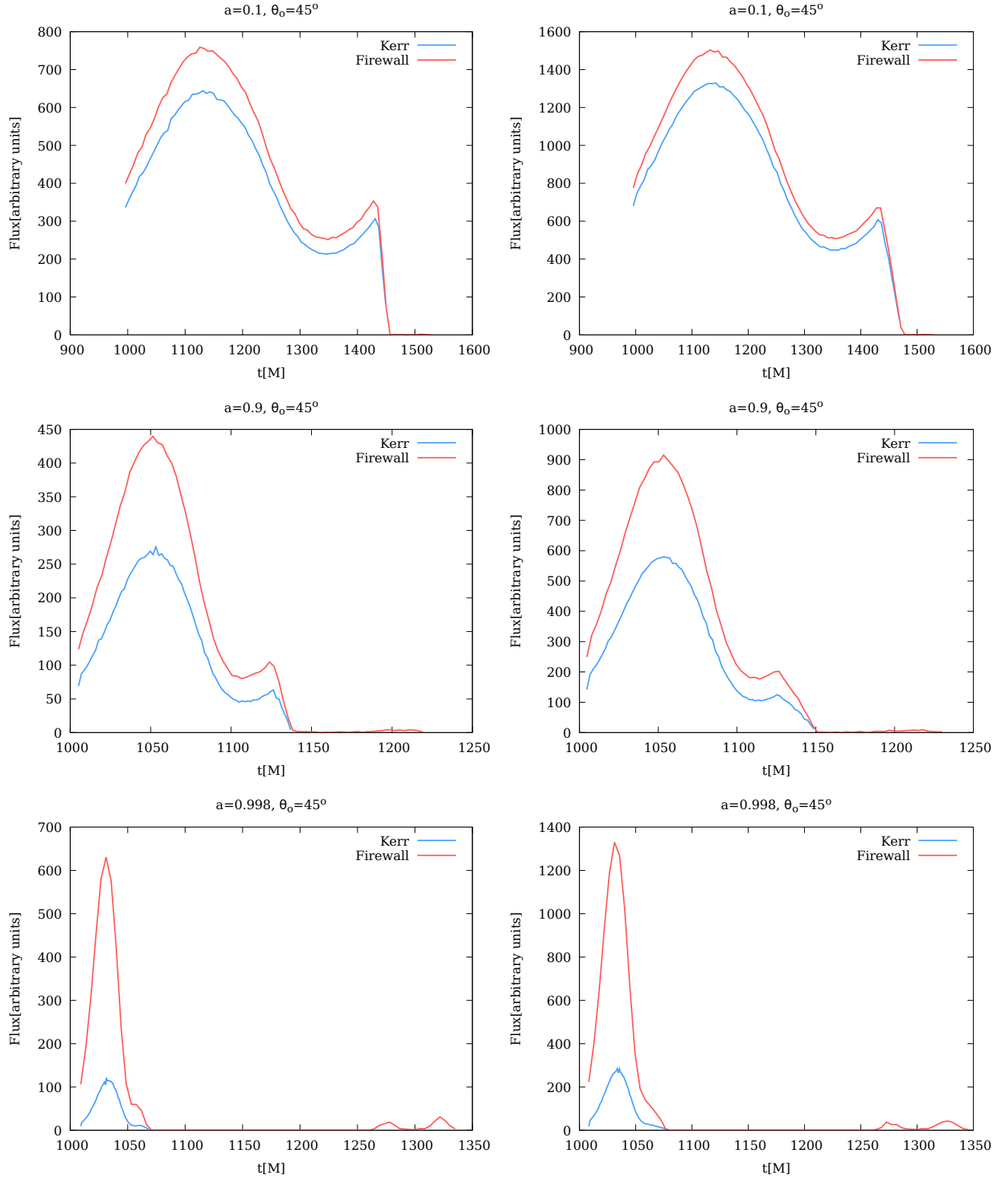


FIG. 3. Comparison of the light curve for hotspot extension, $dr = 0.5M$ (on the left column) and $dr = 1M$ (on the right column). The hotspot location is at radius $r = 3r_{\text{ISCO}}$.

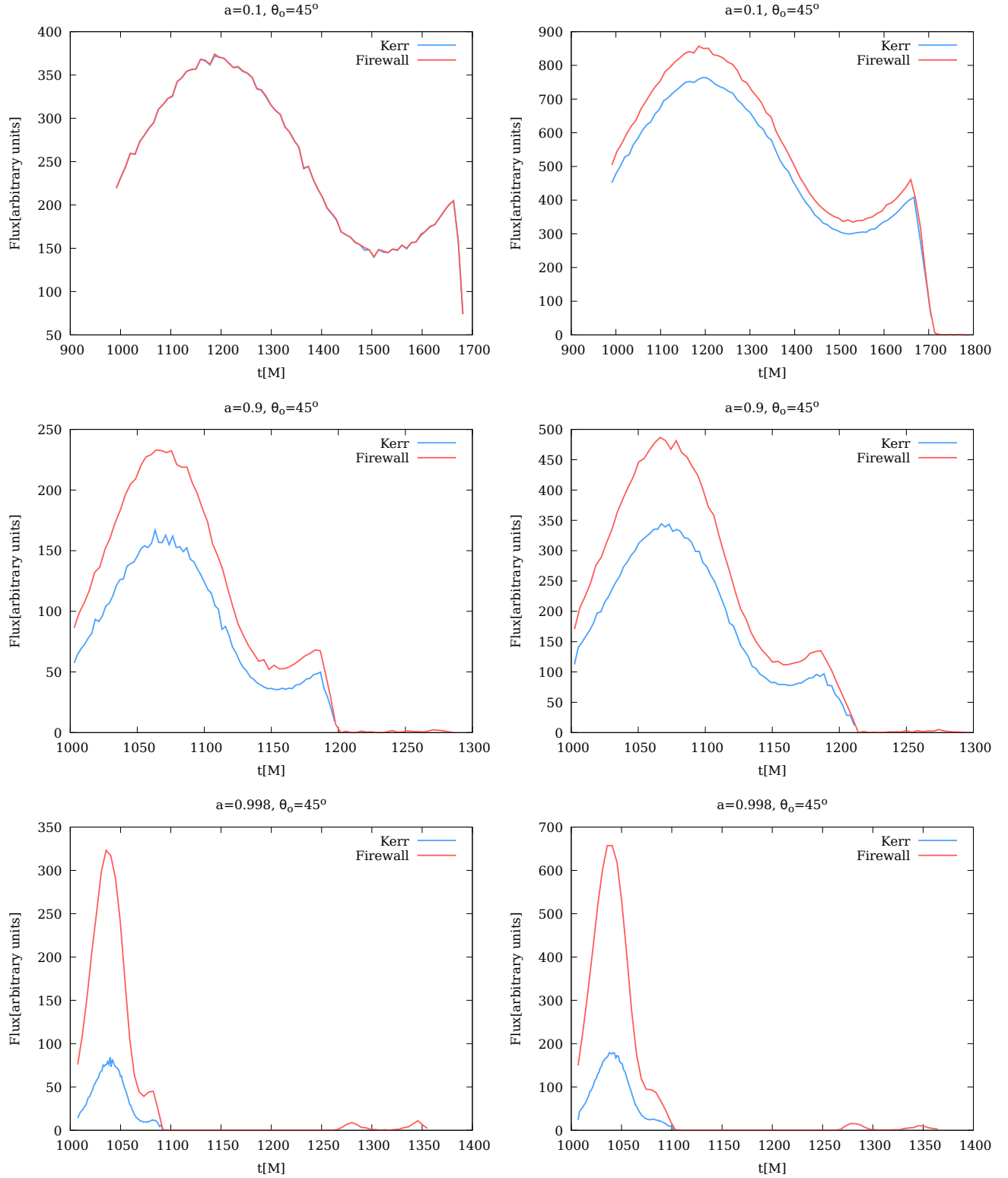


FIG. 4. Comparison of the light curve for hotspot extension, $dr = 0.5M$ (on the left column) and $dr = 1M$ (on the right column). The hotspot location is at radius $r = 4r_{\text{ISCO}}$.

$a \backslash \theta_o$	30°	45°	60°	$a \backslash \theta_o$	30°	45°	60°
0.1	3.25752	3.32353	3.26583	0.1	2.38895	2.49516	2.93629
0.3	2.77288	2.87989	3.19307	0.3	2.76849	3.06709	3.05847
0.5	2.82966	3.26838	3.10464	0.5	3.20562	3.08114	3.25260
0.7	3.08242	3.01541	2.92093	0.7	3.20119	2.98717	2.97302
0.9	3.80323	3.93788	4.17863	0.9	3.88292	3.87944	4.09486
0.998	13.10171	13.16101	13.14078	0.998	12.74827	13.15923	13.11430

TABLE III. Fractional change in the total flux, $\frac{(\text{Total Flux}|_{\text{Firewall}} - \text{Total Flux}|_{\text{Kerr}}) \times 100}{\text{Total Flux}|_{\text{Kerr}}}$ due to reflection of the firewall for hotspot location $r = 3r_{\text{ISCO}}$ with extension, $dr = 0.5M$ (on the left table) and $dr = 1M$ (on the right table).

$a \backslash \theta_o$	30°	45°	60°	$a \backslash \theta_o$	30°	45°	60°
0.1	1.77141	0	0	0.1	2.45035	3.17431	3.13309
0.3	1.23231	2.50167	3.12160	0.3	2.31007	2.05006	2.41707
0.5	2.57008	2.90686	2.58671	0.5	3.02529	2.65849	3.17246
0.7	2.86537	2.74249	3.22768	0.7	2.96613	1.99858	2.47776
0.9	3.85014	4.12945	4.27532	0.9	3.69651	4.02077	4.10031
0.998	12.72629	12.83030	13.08071	0.998	12.65604	12.73300	13.01633

TABLE IV. Fractional change in the total flux, $\frac{(\text{Total Flux}|_{\text{Firewall}} - \text{Total Flux}|_{\text{Kerr}}) \times 100}{\text{Total Flux}|_{\text{Kerr}}}$ due to reflection of the firewall for hotspot location $r = 4r_{\text{ISCO}}$ with extension, $dr = 0.5M$ (on the left table) and $dr = 1M$ (on the right table).

black hole case and the firewall case for the plots of the light curves of a hotspot orbiting in a Keplerian orbit on the equatorial plane is shown for different configurations of the orbital location, spin of the black hole, inclination of the observer and the radial extension of the hotspot in Fig. 1, Fig. 2, Fig. 3 and Fig. 4.

We see that if we increase the spin then for higher value of spin a tail in the observed light curve appears at late time. The possible reason for this is because at larger value of spin the distance between the hotspot and the firewall decreases significantly. It in-fact closes down larger solid angle of the hotspot from which photon may hit the firewall. So one can say that some fraction of the reflected photon in this case would take longer time and appear at the late time in the detector. Effect of firewall with the inclination is not clear from the table at least in our model and further study is required. The fractional change in the total observed flux is presented in the Table. I, Table. II, Table. III and Table. IV for orbital location $r_{\text{ISCO}}, 2r_{\text{ISCO}}, 3r_{\text{ISCO}}, 4r_{\text{ISCO}}$ respectively. We can see the fractional change in the observed flux is a few percents in our model.

As peak of the light curve both in the case of Kerr black holes and firewall appears almost at the same time so one can think of matching this two curve by choosing tuning normalization factor I_0 , local emission profile and the orbital location of the hotspot. Even if the peak is matched but in the case of firewall observer would not only receive more radiation but also observe radiation for longer time. This feature would break the degeneracy between whether the hotspot does have different microphysics of radiation, orbital location and the presence of a firewall.

We would like to stress that although a sophisticated quantitative study is necessary to investigate real astrophysical scenario but this analysis considering a toy model has the merit to indicate new features which appears due to the presence of firewall in the light curve. A more detail study in this direction would be done in a future work.

6. ACKNOWLEDGEMENT

S.H, J.S and Z.S would like to thank the Institute of Physics, Silesian University in Opava for the institutional support provided during this work. This work was supported by the Student Grant Foundation of the Silesian University in Opava, Grant No. SGF/2/2021, which was realized within the EU OPSRE project entitled "Improving the quality of the internal grant scheme of the Silesian University in Opava", reg. number: CZ.02.2.69/0.0/0.0/19_073/0016951. Authors would like to thank Enrico Barausse for his valuable comments.

-
- [1] Abbott et. al. Observation of gravitational waves from a binary black hole merger. *Physical Review Letters*, 116(6), Feb 2016.
 - [2] Kazunori Akiyama et al. First M87 Event Horizon Telescope Results. I. The Shadow of the Supermassive Black Hole. *Astrophys. J. Lett.*, 875:L1, 2019.
 - [3] Kazunori Akiyama et al. First M87 Event Horizon Telescope Results. II. Array and Instrumentation. *Astrophys. J. Lett.*, 875(1):L2, 2019.
 - [4] Kazunori Akiyama et al. First M87 Event Horizon Telescope Results. III. Data Processing and Calibration. *Astrophys. J. Lett.*, 875(1):L3, 2019.
 - [5] Kazunori Akiyama et al. First M87 Event Horizon Telescope Results. IV. Imaging the Central Supermassive Black Hole. *Astrophys. J. Lett.*, 875(1):L4, 2019.
 - [6] Kazunori Akiyama et al. First M87 Event Horizon Telescope Results. V. Physical Origin of the Asymmetric Ring. *Astrophys. J. Lett.*, 875(1):L5, 2019.
 - [7] Kazunori Akiyama et al. First M87 Event Horizon Telescope Results. VI. The Shadow and Mass of the Central Black Hole. *Astrophys. J. Lett.*, 875(1):L6, 2019.
 - [8] Kazunori Akiyama et al. First M87 Event Horizon Telescope Results. VII. Polarization of the Ring. *Astrophys. J. Lett.*, 910(1):L12, 2021.
 - [9] Kazunori Akiyama et al. First M87 Event Horizon Telescope Results. VIII. Magnetic Field Structure near The Event Horizon. *Astrophys. J. Lett.*, 910(1):L13, 2021.
 - [10] S. W. Hawking. Particle Creation by Black Holes. *Commun. Math. Phys.*, 43:199–220, 1975. [Erratum: *Commun.Math.Phys.* 46, 206 (1976)].
 - [11] Ahmed Almheiri, Donald Marolf, Joseph Polchinski, and James Sully. Black Holes: Complementarity or Firewalls? *JHEP*, 02:062, 2013.
 - [12] M. A. Abramowicz, G. Bao, A. Lanza, and X. H. Zhang. X-ray variability power spectra of active galactic nuclei. *Astronomy and Astrophysics*, 245:454, May 1991.
 - [13] G. Bao. The signature of corotating spots in accretion disks. *Astronomy and Astrophysics*, 257(2):594–598, April 1992.
 - [14] Z. Stuchlik and G. Bao. Radiation from hot spots orbiting an extreme Reissner-Nordstrom black hole. *Gen. Rel. Grav.*, 24:945–957, 1992.
 - [15] GRAVITY Collaboration: Abuter, R., Amorim, A., et al. Detection of orbital motions near the last stable circular orbit of the massive black hole sgrA*. *A&A*, 618:L10, 2018.
 - [16] A. F. Zakharov. On the hotspot near a Kerr black hole: Monte-Carlo simulations. *Monthly Notices of the Royal Astronomical Society*, 269(2):283–288, 07 1994.
 - [17] Jeremy Schnittman and Edmund Bertschinger. A Hot Spot Model for Black Hole QPOs. In Philip Kaaret, Frederick K. Lamb, and Jean H. Swank, editors, *X-ray Timing 2003: Rossi and Beyond*, volume 714 of *American Institute of Physics Conference Series*, pages 40–43, July 2004.
 - [18] Mateusz Ruszkowski. X-ray iron line variability for the model of an orbiting flare above a black hole accretion disc. *Monthly Notices of the Royal Astronomical Society*, 315(1):1–10, June 2000.
 - [19] V. Karas. Light Curve of a Source Orbiting a Black Hole: A Fitting Formula. *Astrophysical Journal*, 470:743, October 1996.
 - [20] Alexander Zakharov. On the Hot Spot near a Kerr Black Hole. In Hans Böhringer, Gregor E. Morfill, and Joachim E. Trümper, editors, *Seventeenth Texas Symposium on Relativistic Astrophysics and Cosmology*, volume 759, page 550, January 1995.
 - [21] T. Pečáček, M. Dovčiak, and V. Karas. Power spectra from ‘spotted’ accretion discs. *Astronomische Nachrichten*, 327(10):957, December 2006.
 - [22] Jun Fukue. Light-Curve Diagnosis of a Hot Spot for Accretion-Disk Models. *Publications of the Astronomical Society of Japan*, 55:1121–1125, December 2003.
 - [23] G. Bao, P. Hadrava, and E. Ostgaard. Multiple Images and Light Curves of an Emitting Source on a Relativistic Eccentric Orbit around a Black Hole. *Astrophysical Journal*, 425:63, April 1994.
 - [24] Zilong Li and Cosimo Bambi. Distinguishing black holes and wormholes with orbiting hot spots. *Phys. Rev. D*, 90:024071, 2014.
 - [25] C. T. Cunningham and James M. Bardeen. The Optical Appearance of a Star Orbiting an Extreme Kerr Black Hole. *Astrophysical Journal*, 183:237–264, July 1973.